Low-energy nucleon-deuteron scattering

C. R. Chen and G. L. Payne
Department of Physics and Astronomy, University of Iowa, Iowa City, Iowa 52242

J. L. Friar and B. F. Gibson
Theoretical Division, Los Alamos National Laboratory, Los Alamos, New Mexico 87545
(Received 6 July 1988)

The configuration-space Faddeev equations for the nucleon-deuteron scattering problem are solved for energies below the three-body breakup threshold. We extract the *s*-wave scattering lengths from fits to the calculated effective range functions, and the results are in good agreement with our previous zero-energy calculations. For the *pd*-doublet case we find a pole at negative energies which lies closer to the physical region than that for the *nd*-doublet case. Our calculated phase shifts fall within the existing experimental error bars, suggesting that accurate experiments for scattering energies below 0.3 MeV are necessary in order to obtain a reliable experimental estimate of the *pd*-doublet scattering length.

I. INTRODUCTION

Few-body systems such as the trinucleons, for which the nonrelativistic model Hamiltonian can be solved exactly, provide fundamental tests of our understanding of nuclear interactions. Direct comparison of model calculations with experimental data is feasible. In addition, they can also be used as a testing ground in which one searches for novel features of physical observables. The three-body bound-state problem has been solved by several groups,[1–6] and it is encouraging that these different groups now agree on the numerical results for the same model Hamiltonians. However, it has been discouraging to find that most of the bound-state properties scale with the trinucleon binding energies.[7] That is, different phenomenological potentials which yield the same trinucleon binding energy predict nearly the same charge radii, asymptotic normalization constants, magnetic moments, etc. It is the three-body scattering problem which offers us a separate opportunity to explore, in depth, the accuracy of our knowledge of the nuclear interactions.

Nucleon-deuteron scattering at zero energy, which can be separated into (total) spin doublet and quartet configurations, is the simplest three-nucleon scattering system which can be characterized by a single observable, the scattering length. Experimentally, the neutron-deuteron (*nd*) scattering lengths have been reasonably well determined using 130 eV neutrons.[8] The generally accepted values are

$$^4a_{nd} = 6.35 \pm 0.02 \text{ fm}$$

and

$$^2a_{nd} = 0.65 \pm 0.04 \text{ fm} .$$

The proton-deuteron (*pd*) scattering data[9–11] are known less precisely because the Couloumb barrier greatly suppresses the cross section (much of which is pure Coulomb in nature), and exist only for energies above 0.4 MeV. The zero-energy *pd* scattering lengths were obtained by extrapolation from the available low-energy data. The reported doublet scattering lengths ($^2a_{pd}$) are 1.3 ± 0.2 fm (Ref. 9), 2.73 ± 0.10 fm (Ref. 10), and $4.00 + 1.00/-0.67$ fm (Ref. 11). The experimental agreement is much better for the spin-quartet configuration, and the values of $^4a_{pd}$ cluster around 11.5 fm (Refs. 9–11).

On the theoretical side, the correlation discovered by Phillips[12] between $^2a_{nd}$ and the triton binding energy is now well established. Most model results fall on the so-called Phillips line, which passes through the experimental data. Furthermore, all nucleon-nucleon (*NN*) interactions reproduce the experimental value of $^4a_{nd}$. Because the Pauli principle makes the (effective) quartet *nd* interaction repulsive at short distances, $^4a_{nd}$ is sensitive primarily to the asymptotic properties of the deuteron (the binding energy) and the tail of the spin-triplet *NN* interaction. The situation is not as clear in the case of the *pd* scattering lengths. Avishai *et al.*,[13] using an approximate procedure, Timm *et al.*,[14] using a Jost function analysis, and Eyre *et al.*,[15] using a dispersion relation analysis, all reproduced the quartet difference $^4a_{pd} - {}^4a_{nd}$. Later work by Kvitsinskii,[16] using the MT I-III potential,[17] also gave results which agree very well with both the published doublet and quartet experimental values. On the other hand, Alt[18] used an *s*-wave separable potential to obtain $^4a_{pd} = 13.3$ fm. Our own MT I-III calculations found $^4a_{pd}$ to be approximately 14 fm, and $^2a_{pd}$ to be approximately zero.[19] Additional calculations by other groups, which have recently been reported, agree with our results.[20–22] The discrepancy between theory and experiment was further explored using more realistic *NN* potentials,[23] and with a combination of *NN* and three-nucleon potentials.[24] From these extensive studies, it was found that a correlation still exists between $^2a_{pd}$ and the ^{3}He binding energy. This *pd* Phillips line, though far from being straight, has the same general behavior as the

 ©1989 The American Physical Society

original *nd* Phillips line, and its existence has been confirmed by other groups.[21,22] The essential question remains: Why does the experimental datum lie far off our *pd* Phillips line?

Much effort has gone into trying to understand the source of the differences among the various *pd* calculations. Of special concern were differences between our results and those of Kvitsinskii, because in both calculations the configuration-space Faddeev equations for the MT I-III potential model were solved. One primary difference is that our own calculations were done for (exactly) zero energy, while all other groups worked at nonzero energies and extrapolated their results to zero energy. This cannot itself be the source of the disagreement if it is possible to perform the extrapolation accurately. Thus, we were motivated to solve the *pd* scattering problem for energies ranging from zero to just below that for (threshold) breakup of the deuteron.

Recently, a concern has been raised about the Coulomb polarization potential in low-energy *pd* scattering. Kvitsinskii and Merkuriev[25] reported that the polarization could affect the doublet effective range significantly for energies up to about 1 MeV, whereas the quartet effective range is affected only for energies below 10 keV. However, Berthold and Zankel[21] found that the Coulomb polarization potential was negligible for the entire energy range of their study (down to 0.2 MeV). A more recent investigation[26] has shown that the effect of the polarization potential in a two-body model is significant only for energies less than 5 keV, and that the scattering length calculated at zero energy without the polarization potential is a good approximation so long as the boundary conditions are enforced at distances less than several hundred fm. Recently, Adhikari and Das[27] have confirmed these two-body model results using a potential which generates more realistic *nd* and *pd* scattering lengths. For these reasons the polarization potential is neglected in this work.

One possible source of the disagreement between theoretical results obtained at zero energy, and theoretical and experimental results obtained by extrapolating from higher energies, is a pole in the effective range function near threshold. Such a pole could lead to significant curvature in that function at low energies which could make the extrapolation unreliable. Although the existence of a pole term in the effective range function for *pd* doublet scattering was not supported by the results of the experimental analysis,[9–11] we find the pole to be very apparent in our numerical results. Moreover, Berthold and Zankel[21] found that including a pole was essential for a proper understanding of their doublet scattering results. Our *pd* doublet effective range function exhibits large curvature for energies less than a few hundred keV. Such a large curvature in the calculated effective range function at low energies was also found in Ref. 22; this is presumably the effect of just such a pole. This indicates that caution must be exercised when extrapolating to zero energy.

In Sec. II of this paper we outline the configuration-space three-body scattering equations for energies below the threshold for breakup of the deuteron. We choose to work in configuration space because the long-range Coulomb force is easily handled in that space. We present our numerical results and analyses together with the experimental numbers in Sec. III. In Sec. IV we summarize our conclusions.

II. CONFIGURATION-SPACE FORMALISM

The Faddeev equations[28] were introduced because the Lippmann-Schwinger equation fails to yield a unique solution.[29] Noyes first outlined the configuration-space boundary condition problem for *nd* scattering.[30] Inclusion of the long-range Coulomb interaction is straightforward in configuration space for energies below the deuteron breakup threshold. For higher energies, both the *nd* and *pd* boundary conditions are much more complicated. Therefore, in this paper we limit our consideration to energies below the three-body breakup threshold. We base our work on the approach that we previously employed, both for the zero-energy scattering problem and for the bound-state problem.

We have modified our zero-energy configuration-space Faddeev code[23] to treat scattering energies up to the deuteron breakup threshold The Hamiltonian of the system in the center-of-mass (c.m.) frame is

$$H=T+V(\vec{x}_1)=V(\vec{x}_2)+V(\vec{x}_3)+V^C(x_1,x_2,x_3)\ , \tag{1}$$

where

$$V^C(x_1,x_2,x_3)=\sum_{i=1}^{3}\frac{e^2}{x_i}\frac{[1+\tau_z(j)][1+\tau_z(k)]}{4} \tag{2}$$

is a sum over two-body Coulomb interactions, and $V(\vec{x}_i)$ is the NN potential acting between particles j and k. We use the Jacobi coordinates

$$\vec{x}_i=\vec{r}_j-\vec{r}_k$$

and (3)

$$\vec{y}_i=\tfrac{1}{2}(\vec{r}_j+\vec{r}_k)-\vec{r}_i\ ,$$

where i, j, and k imply cyclic permutation.

The total energy of the system in the c.m. frame is the sum of the deuteron binding energy and the kinetic energy

$$E=E_d+E_{\text{c.m.}}=-\frac{\hbar^2q^2}{M}+\frac{3\hbar^2k^2}{4M}=-\frac{\hbar^2\kappa^2}{M}\ , \tag{4}$$

where M is the nucleon mass, q is the two-body bound-state wave number, and k is the momentum of the incident nucleon in the c.m. frame. Note that the nucleon kinetic energy in the lab frame is $\frac{3}{2}$ times the corresponding energy in the c.m. frame. The former is usually quoted in experimental papers.

The total wave function Ψ is written as the sum of three Faddeev amplitudes

$$\Psi=\psi(\vec{x}_1,\vec{y}_1)+\psi(\vec{x}_2,\vec{y}_2)+\psi(\vec{x}_3,\vec{y}_3)=\psi_1+\psi_2+\psi_3\ . \tag{5}$$

The Schrödinger equation is then decomposed into three Faddeev equations

$$[T+V(\vec{x}_i)+V^C-E]\psi_i+V(\vec{x}_i)(\psi_j+\psi_k)=0 \ . \quad (6)$$

For identical particles we need to solve only the $i=1$ equation, because all the functions ψ_i have the same functional form. For the partial-wave representation of the Faddeev amplitudes, we use the j-J coupling scheme and write ψ_i in the form

$$\psi_i=\sum_\alpha \frac{\psi_\alpha(x_i,y_i)}{x_i y_i}|\alpha\rangle_i \ , \quad (7)$$

where

$$|\alpha\rangle_i=|[(l_\alpha,s_\alpha)j_\alpha,(L_\alpha,S_\alpha)J_\alpha]JM;(t_\alpha,T_\alpha)TM_T\rangle$$

labels different channels and i indicates that the order of coupling is $[(j,k),i]$. The relative orbital angular momentum of the j-k pair is l_α, s_α is the spin of the j-k pair, j_α is the total angular momentum of the j-k pair, L_α is the orbital angular momentum of particle i relative to the c.m. of the j-k pair, S_α is the spin of particle i ($S_\alpha=\frac{1}{2}$), J_α is the total angular momentum of particle i, J is the total angular momentum of the system, t_α is the isospin of the j-k pair, T_α is the isospin of particle i ($T_\alpha=\frac{1}{2}$), and T is the total isospin of the system. We neglect the $T=\frac{3}{2}$ component, since it has been shown to make a very small contribution.[19]

To investigate the validity of the extrapolation from low energies to zero energy, we use the MT I-III potential as our model NN interaction. However, the following formalism is valid for any of the more realistic NN potentials, or NN and three-nucleon potentials together. Phase shifts for p waves, etc., can be obtained as well. Nevertheless, we concentrate on the s-wave results in this work. We use the MT I-III model parameters given in Ref. 1, which are slightly different from the parameters in Ref. 17. With this s-wave potential there is no tensor-force coupling, only a single channel remains in the description of the quartet configuration, and the doublet case requires only two channels. The quantum numbers of each channel are listed in Table I. The first channel of the doublet state is "closed", because the scattering energy is insufficient to break up the deuteron. Other channels are "open."

We multiply Eq. (6) by x_1y_1, take the inner product with ${}_1\langle\alpha|$, and then transform to the hyperspherical variables defined by

$$x_1=\rho\cos\theta$$

and (8)

$$y_1=\frac{\sqrt{3}}{2}\rho\sin\theta \ .$$

The resulting equations are

$$(\Delta_\alpha-\kappa^2)\psi_\alpha(\rho,\theta)-\sum_{\alpha'}(v_{\alpha\alpha'}+v^C_{\alpha\alpha'})\psi_{\alpha'}(\rho,\theta)$$
$$-\sum_{\alpha''}v_{\alpha\alpha''}\sum_{\alpha'}\int_{\theta^-}^{\theta^+}d\theta' K_{\alpha''\alpha'}(\theta,\theta')\psi_{\alpha'}(\rho,\theta')=0 \ , \quad (9)$$

where κ is defined in Eq. (4), and

TABLE I. The two channel states for the doublet system ($J=\frac{1}{2}$) and the single channel for the quartet system ($J=\frac{3}{2}$).

J	α	$(l_\alpha,s_\alpha)\ j_\alpha$	$(L_\alpha,S_\alpha)\ J_\alpha$	t_α
$\frac{1}{2}$	1	(0,0) 0	$(0,\frac{1}{2})\ \frac{1}{2}$	1
	2	(0,1) 1	$(0,\frac{1}{2})\ \frac{1}{2}$	0
$\frac{3}{2}$	1	(0,1) 1	$(0,\frac{1}{2})\ \frac{1}{2}$	0

$$v_{\alpha\alpha'}=\frac{M}{\hbar^2}{}_1\langle\alpha|V(\vec{x}_1)|\alpha'\rangle_1 \ ,$$
$$v^C_{\alpha\alpha'}=\frac{M}{\hbar^2}{}_1\langle\alpha|V^C(x_1,x_2,x_3)|\alpha'\rangle_1 \ ,$$
$$\sum_{\alpha'}\int_{\theta^-}^{\theta^+}d\theta' K_{\alpha''\alpha'}(\theta,\theta')\psi_{\alpha'}(\rho,\theta')=x_1y_1{}_1\langle\alpha''|\psi_2+\psi_3\rangle \ , \quad (10)$$
$$\Delta_\alpha=\frac{\partial^2}{\partial\rho^2}+\frac{1}{\rho}\frac{\partial}{\partial\rho}+\frac{1}{\rho^2}\frac{\partial^2}{\partial\theta^2}-\frac{l_\alpha(l_\alpha+1)}{\rho^2\cos^2\theta}-\frac{L_\alpha(L_\alpha+1)}{\rho^2\sin^2\theta} \ .$$

The integration limits are the same as for the bound-state calculations.[1]

Following the same procedures as for the zero-energy scattering problem,[23] we separate the outgoing wave Ω_α from the known incident wave ϕ_α:

$$\psi_\alpha(x_1,y_1)=\phi_\alpha(x_1,y_1)+\Omega_\alpha(x_1,y_1) \ . \quad (11)$$

For the closed channels, $\phi_\alpha=0$. For the open channels,

$$\phi_\alpha(x_1,y_1)=y_1I_{L_\alpha}(y_1)u_\alpha(x_1) \ , \quad (12)$$

where $u_\alpha(x_1)$ is the reduced deuteron bound-state wave function. With the usual Coulomb parameters $\zeta=ky_1$ and $\eta=2Me^2/3\hbar^2k$, I_L is related to the regular Coulomb wave function[31] F_L by

$$I_L(y_1)=\frac{F_L(\eta,\zeta)}{\zeta C_L(\eta)} \ , \quad (13)$$

where the factors C_L are

$$C_L(\eta)=\frac{(L^2+\eta^2)^{1/2}}{L(2L+1)}C_{L-1}(\eta) \ ,$$
$$C_0^2(\eta)=\frac{2\pi\eta}{e^{2\pi\eta}-1} \ . \quad (14)$$

For large values of y_1, the outgoing wave Ω_α has the asymptotic form

$$\Omega_\alpha(x_1,y_1)\xrightarrow[y_1\to\infty]{}-t_\alpha K_{L_\alpha}(y_1)u_\alpha(x_1) \ , \quad (15)$$

for the open channels, where

$$K_L(y_1)=(2L+1)k^LC_L(\eta)G_L(\eta,\zeta) \ , \quad (16)$$

and G_L is the irregular Coulomb wave function. The scattering length, a, is defined as the limit of t_α in Eq. (15) as k goes to zero. For the closed channels, the outgoing wave approaches zero in the asymptotic regions.

A useful quantity which can be checked against experimental data is the phase shift, δ_L. This can be calculated easily from the asymptotic wave functions for the open channels,

$$\psi_\alpha(x_1,y_1)\xrightarrow[y_1\to\infty]{}\left[\frac{F_{L_\alpha}(\eta,\xi)}{kC_{L_\alpha}(\eta)}-t_\alpha(2L_\alpha+1)k^{L_\alpha}C_{L_\alpha}(\eta)G_{L_\alpha}(\eta,\xi)\right]u_\alpha(x_1)$$
$$=\frac{1}{kC_{L_\alpha}(\eta)}[F_{L_\alpha}(\eta,\xi)+\tan\delta_{L_\alpha}G_{L_\alpha}(\eta,\xi)]u_\alpha(x_1)\ , \quad (17)$$

Thus, the phase shifts are related to the quantity t_α by

$$\tan\delta_{L_\alpha}(k)=-(2L_\alpha+1)t_\alpha k^{L_\alpha+1}C^2_{L_\alpha}(\eta)\ . \quad (18)$$

We factor out the deuteron wave function from Ω_α, so that the unknown function to be calculated is smoother. The auxiliary function A_α is defined by

$$\Omega_\alpha(x_1,y_1)=A_\alpha(\rho,\theta)\frac{u_\alpha(x_1)}{x_1}\ , \quad (19)$$

for the open channels and

$$\Omega_\alpha(x_1y_1)=A_\alpha(\rho,\theta)e^{-\kappa\rho}\ , \quad (20)$$

for the closed channels. Note that we do not factor out the irregular Coulomb wave function in Eq. (19) for the open channels, because the nodes of G_L imply that it cannot easily be removed. The factor of $1/x_1$ is included to simplify the boundary conditions at $x_1=0$.

Substituting Eq. (11) into Eq. (9) and using Eqs. (19) and (20), one obtains the following differential equations for the open channels:

$$\frac{u_\alpha}{x_1}\left[\frac{\partial^2A_\alpha}{\partial\rho^2}+\frac{1}{\rho}\frac{\partial A_\alpha}{\partial\rho}+\frac{1}{\rho^2}\frac{\partial^2A_\alpha}{\partial\theta^2}\right]+\frac{2}{x_1}\left[\frac{u_\alpha}{x_1}-u'_\alpha\right]\left[\frac{A_\alpha}{x_1}-\frac{\partial A_\alpha}{\partial x_1}\right]$$
$$+\frac{3}{4}\left[k^2-\frac{L_\alpha(L_\alpha+1)}{y_1^2}\right]A_\alpha\frac{u_\alpha}{x_1}+\frac{A_\alpha}{x_1}\sum_{\alpha'}v_{\alpha\alpha'}u_{\alpha'}-\sum_{\alpha'}(v_{\alpha\alpha'}+v^C_{\alpha\alpha'})A_{\alpha'}\frac{u_{\alpha'}}{x_1}$$
$$-\sum_{\alpha''}v_{\alpha\alpha''}\sum_{\alpha'}\int_{\theta^-}^{\theta^+}d\theta' K_{\alpha''\alpha'}(\theta,\theta')\Omega_{\alpha'}(\rho,\theta')=\sum_{\alpha'}(v^C_{\alpha\alpha'}-\omega\delta_{\alpha\alpha'})\phi_{\alpha'}+\sum_{\alpha''}v_{\alpha\alpha''}\sum_{\alpha'}\int_{\theta^-}^{\theta^+}d\theta' K_{\alpha''\alpha'}(\theta,\theta')\phi_{\alpha'}(\rho,\theta')\ , \quad (21)$$

where $\omega=Me^2/\hbar^2y_1$ and $u'_\alpha\equiv du_\alpha/dx_1$. For the closed channels we have

$$\left[\Delta_\alpha-\frac{\kappa}{\rho}\right]A_\alpha-2\kappa\frac{\partial A_\alpha}{\partial\rho}-\sum_{\alpha'}(v_{\alpha\alpha'}+v^C_{\alpha\alpha'})A_{\alpha'}-\sum_{\alpha''}v_{\alpha\alpha''}\sum_{\alpha'}\int_{\theta^-}^{\theta^+}d\theta' K_{\alpha''\alpha'}(\theta,\theta')e^{\kappa\rho}\Omega_{\alpha'}(\rho,\theta')$$
$$=\sum_{\alpha''}v_{\alpha\alpha''}\sum_{\alpha'}\int_{\theta^-}^{\theta^+}d\theta' K_{\alpha''\alpha'}(\theta,\theta')e^{\kappa\rho}\phi_{\alpha'}(\rho,\theta')\ . \quad (22)$$

The boundary conditions for $A_\alpha(\rho,\theta)$ are

$$A_\alpha(0,\theta)=A_\alpha(\rho,0)=A_\alpha(\rho,\pi/2)=0 \quad (23)$$

for all channels,

$$A_\alpha(\rho,\theta)\xrightarrow[y_1\to\infty]{}-t_\alpha x_1K_{L_\alpha}(y_1) \quad (24)$$

for the open channels, and

$$A_\alpha(\rho,\theta)\xrightarrow[\rho\to\infty]{}\text{const} \quad (25)$$

for the closed channels. These boundary conditions are implemented by requiring that at $\rho=\rho_{\max}$,

$$\frac{\partial A_\alpha}{\partial\rho}=\cos\theta\frac{A_\alpha}{x_1}+\frac{\sqrt{3}}{2}\sin\theta\frac{A_\alpha}{K_{L_\alpha}}\frac{\partial K_{L_\alpha}}{\partial y_1} \quad (26)$$

for the open channels, and

$$\frac{\partial A_\alpha}{\partial\rho}=0 \quad (27)$$

for the closed channels.

To solve for $A_\alpha(\rho,\theta)$ we use a spline expansion

$$A_\alpha(\rho,\theta)=\sum_{i,j}a^\alpha_{ij}S_i(\rho)S_j(\theta)\ , \quad (28)$$

where we choose to use the bicubic Hermite splines.[32] We then solve for the unknown coefficients a^α_{ij} by the technique of orthogonal collocation.[32]

III. RESULTS AND ANALYSES

The grids for the variables ρ and θ are generated in the same way as in our previous investigations. The details

TABLE II. The s-wave phase shifts as a function of the scattering energies in the center-of-mass system. The energies are in MeV and the phase shifts are in degrees.

$E_{c.m.}$	$^4\delta_{nd}$	$^2\delta_{nd}$	$^4\delta_{pd}$	$^2\delta_{pd}$
0.001	−2.09	−0.230	0.0	0.0
0.05	−14.6	−1.99	−2.69	−0.113
0.1	−20.4	−3.28	−7.46	−0.537
0.2	−28.3	−5.68	−15.6	−1.96
0.3	−34.0	−7.95	−21.9	−3.73
0.4	−38.5	−10.1	−27.0	−5.62
0.5	−42.4	−12.1	−31.3	−7.53
0.6	−45.7	−14.0	−35.1	−9.40
0.7	−48.6	−15.8	−38.4	−11.2
0.8	−51.2	−17.5	−41.4	−13.0
0.9	−53.6	−19.1	−44.1	−14.6
1.0	−55.8	−20.7	−46.5	−16.2

of how to search for optimal values of the parameters can be found in Ref. 23. In this paper, we present only the values of the parameters used and the results of our calculations. The parameters that we vary to ensure an accurate numerical solution are: the numbers and distributions of the ρ and θ points, and the value of ρ_{max} beyond which we assume that the wave function has achieved its asymptotic form. The ρ points are distributed uniformly between 0 and 1 fm, scaled by a factor of $S_\rho=1.3$ between 1 and 12 fm, and equally spaced between 12 fm and ρ_{max}. The θ points are distributed uniformly between 0 and $\pi/6$, while scaled by a factor of $S_\theta=1.3$ between $\pi/6$ and $\pi/2$ in order to ensure that more points are concentrated in the region where the wave function has the most structure. We found $\rho_{max}=60$ fm to be satisfactory throughout the entire study. The numbers of ρ points used were 4, 8, and 10 in the interior, midrange, and exterior regions, respectively. The *pd* quartet results were generated using 12 points in the exterior region. The numbers of θ points were 17 and 3 in the regions $\pi/6$ to $\pi/2$, and 0 to $\pi/6$, respectively.

The effective range function for *nd* scattering is defined by

$$K(E)=k\cot\delta_0(k)\ . \tag{29}$$

For *pd* scattering, it is given by

$$K(E)=C_0^2(\eta)k\cot\delta_0(k)+2k\eta h(\eta)\ , \tag{30}$$

where $C_0^2(\eta)$ is defined in Eq. (14), and

$$h(\eta)=-\ln(\eta)+\mathrm{Re}\psi(1+i\eta)\ ,$$

with ψ denoting the digamma function.[31] The s-wave phase-shift, δ_0, defined in Eq. (17), will have different numerical values for the Coulomb (*pd*) and non-Coulomb (*nd*) cases. Because we match to Coulomb asymptotic functions in the *pd* case, δ_0 vanishes in the absence of a strong potential, as it does in the *nd* case. In Table II we list the s-wave phase-shift results for all four cases. The corresponding results for the (modified) effective range functions are separately plotted as a function of $E_{c.m.}$ for the *nd* and *pd*, quartet and doublet cases in Figs. 1–4.

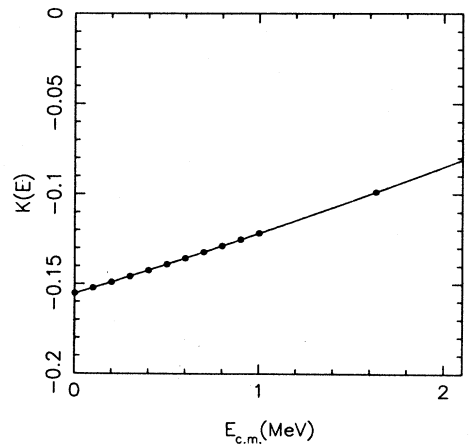

FIG. 1. The effective range function plotted versus the scattering energy in the center-of-mass system for the *nd* quartet scattering; $^4a_{nd}=6.43$ fm.

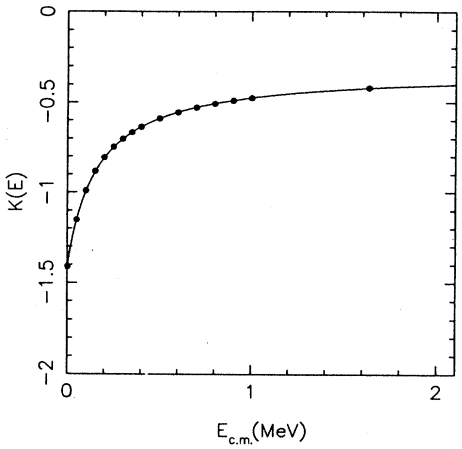

FIG. 2. Same as Fig. 1 but for the *nd* doublet scattering; $^2a_{nd}=0.71$ fm.

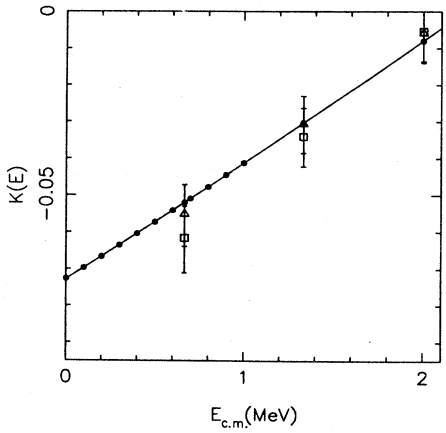

FIG. 3. The effective range function plotted versus the scattering energy in the center-of-mass system for the *pd* quartet scattering. The triangles are the experimental points found from the phase shifts in Ref. 10, and the squares are those from Ref. 11. The error bars reflect the experimental uncertainty of ±2° in the experimental phase shifts. $^4a_{pd}=13.8$ fm.

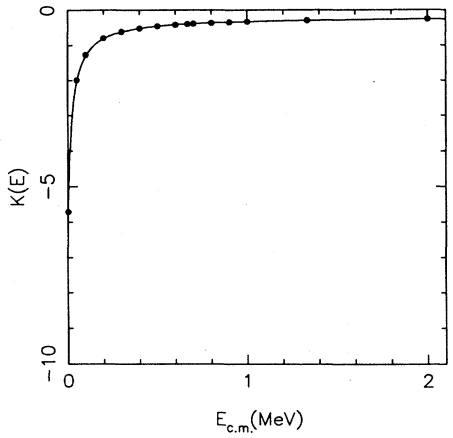

FIG. 4. The effective range function plotted versus the scattering energy in the center-of-mass system for the *pd* doublet scattering; ${}^2a_{pd}=0.17$ fm.

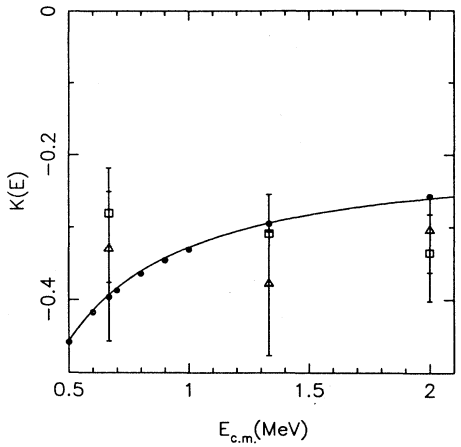

FIG. 5. Expanded plot of Fig. 4 for scattering energies greater than 0.5 MeV. Also plotted are the data from Ref. 10 (triangles) and Ref. 11 (squares). The error bars reflect the experimental uncertainty of $\pm 3°$ in the experimental phase shifts.

The solid dots are our numerical results, and the curves are the fits made by using the effective range formula including a pole in the denominator

$$K(E)=\frac{-\frac{1}{a}+\frac{1}{2}r_0k^2}{1+k^2/k_0^2}\ , \tag{31}$$

where a is the extrapolated scattering length at zero energy.

To check the accuracy of our calculations, we compare our phase shifts to available calculated and experimental numbers. In Table III we compare our *s*-wave *nd* phase shifts with two other theoretical calculations[33,34] for the MT I-III *NN* potential model. The agreement is very good considering that the calculational methods are quite different. Kloet and Tjon[33] used Padé techniques to sum the scattering series, while a noncompact integral equation was solved in Ref. 34. The results for the *pd* *s*-wave phase shifts, compared to the experimental values,[10,11] are illustrated in Table IV. Arvieux[10] analyzed the cross-section data available in 1973, while Huttel *et al.*[11] used additional cross-section data, as well as analyzing power data. The latter work also compares these two phase-shift analyses with model estimates of Alt and Eyre *et al.* Our results fall within the experimental uncertainties, which are about 2° for the quartet phases and about 3° for the doublet phases. We also plot values of the effective range function calculated from the experimental phase shifts in Figs. 3 and 5, where the triangles denote Arvieux's values[10] and the squares are those of Huttle *et al.*[11] Figure 5 is simply part of Fig. 4 plotted using a different scale in order to show the differences between our numerical results and the experimental values.

From the fits to our calculated values, we observe no poles in the $E<0$ region for either *nd* or *pd* quartet scattering: that is, there is no singularity corresponding, for example, to the deuteron binding energy. For the doublet configuration, poles corresponding to three-body virtual bound states were obtained at

$$E_v=-3\hbar^2k_0^2/4M\simeq -160 \text{ keV}$$

in the *nd* case, and at $E_v\simeq -25$ keV in the *pd* case. The presence of the Coulomb force weakens the *pd* interaction and moves the second sheet pole toward the physical region. (This observation was tested by multiplying the Coulomb interaction by a factor of $\frac{1}{2}$ which resulted in $E_v\simeq -85$ keV.) The zero-energy scattering lengths thus obtained for the MT I-III model are

$${}^4a_{nd}=6.43 \text{ fm},$$

$${}^2a_{nd}=0.71 \text{ fm},$$

$${}^4a_{pd}=13.8 \text{ fm},$$

and

$${}^2a_{pd}=0.17 \text{ fm}.$$

These scattering lengths, extrapolated from the low-energy results, agree with our previous zero-energy calculations. It is also clear that one can easily extrapolate to the wrong value of ${}^2a_{pd}$ if one is not aware of the enormous curvature in the effective range function $K(E)$ for $E_{\text{c.m.}}<300$ keV. In other words, taking into account the pole in the *pd* doublet effective range function is essential if one is to extrapolate accurately and extract the correct

TABLE III. Comparison of the *nd* *s*-wave phase shifts with other theoretical results. The energies are in MeV and the phase shifts are in degrees. Note that we have added 180° to the phases in order to compare directly with those of Refs. 33 and 34.

	${}^4\delta_{nd}$			${}^2\delta_{nd}$	
$E_{\text{c.m.}}$	Ours	Ref. 33	Ref. 34	Ours	Ref. 33
1.633	113.3	114.3	113.4	151.4	151.1
2.180	106.4	107.6	106.4	146.4	146.4

TABLE IV. Comparison of the *pd* *s*-wave phase shifts with the experimental values. The energies are in MeV and the phase shifts are in degrees.

	$^4\delta_{pd}$			$^2\delta_{pd}$		
$E_{c.m.}$	Ours	Ref. 10	Ref. 11	Ours	Ref. 10	Ref. 11
0.667	−37.3	−36.6	−35.1	−10.6	−12.6	−14.1
1.333	−53.5	−53.4	−52.5	−21.1	−17.5	−20.4
2.000	−63.8	−64.3	−64.4	−28.8	−25.8	−24.1

scattering length from the low-energy results, for either theoretical or experimental phase shifts. We suggest that experiments be performed at lower energies (if possible) and with improved accuracy in order to examine this effect.

Because we confirm our previous zero-energy scattering lengths, our *pd* Phillips line remains a valid representation of the correlation between $^2a_{pd}$ and the ^{3}He binding energy. Although we use the *s*-wave MT I-III potential in our model calculation, results corresponding to more realistic *NN* potentials, or combinations of *NN* and three-nucleon potentials, are easily obtained. We need only correlate the ^3He binding energies calculated for these models[2,35] with the scattering lengths specified by the Phillips line. In particular, the estimates made in Refs. 23 and 24 for the physical values of $^2a_{pd}$ and $^4a_{pd}$ are still valid.

IV. CONCLUSIONS

We have solved the nucleon-deuteron scattering problem below the three-body breakup threshold. The *s*-wave scattering lengths calculated by extrapolating from the low-energy results are in good agreement with our previous zero-energy results. Both the *nd* and *pd* Phillips lines still provide the empirical relations between the doublet scattering lengths and the trinucleon binding energies. By using numerical fits to the effective range functions, we find that a pole on the negative-energy axis exists for the *pd* doublet configuration, complementing the well-known virtual-state singularity for the *nd* doublet case.[36,37] The pole term or, equivalently, the large curvature of the effective range function in the $E_{c.m.} < 300$ keV region, is almost certainly the source of the disagreement between our zero-energy *pd* doublet scattering length calculation and other calculations as well as with the experimental results. This long conjectured pole was identified in the three-body calculations of Ref. 21, and it was later observed in the effective two-body model calculations of Ref. 22. Accurate experiments with $E_{c.m.} < 300$ keV are necessary in order to extract a valid estimate for the *pd* doublet scattering length.

ACKNOWLEDGMENTS

The work of J.L.F. and B.F.G. was performed under the auspices of the U.S. Department of Energy, while that of G.L.P. was supported in part by that agency. One of us (J.L.F.) would like to thank S. P. Merkuriev and Y. Simonov for suggesting that these calculations would likely resolve the discrepancies that exist.

[1]G. L. Payne, J. L. Friar, B. F. Gibson, and I. R. Afnan, Phys. Rev. C **32**, 823 (1980).
[2]C. R. Chen, G. L. Payne, J. L. Friar, and B. F. Gibson, Phys. Rev. C **31**, 2266 (1985); this reference compares the results of many of the available calculations.
[3]C. Hajduk and P. U. Sauer, Nucl. Phys. **A369**, 321 (1981); P. U. Sauer, Prog. Nucl. Phys. **16**, 35 (1986).
[4]S. Ishikawa, T. Sasakawa, T. Sawada, and T. Ueda, Phys. Rev. Lett. **53**, 1877 (1984); T. Sasakawa and S. Ishikawa, Few-Body Syst. **1**, 3 (1986).
[5]A. Bömelburg, Phys. Rev. C **28**, 403 (1983).
[6]I. R. Afnan and N. D. Birrell, Phys. Rev. C **16**, 823 (1977); J. Chauvin, C. Gignoux, J. J. Benayoun, and A. Laverne, Phys. Lett. **78B**, 5 (1978).
[7]J. L. Friar, B. F. Gibson, G. L. Payne, and C. R. Chen, Phys. Lett. **161B**, 241 (1985).
[8]W. Dilg, L. Koester, and W. Nistler, Phys. Lett. **36B**, 208 (1971).
[9]W. T. H. van Oers and K. W. Brockman, Jr., Nucl. Phys. **A92**, 561 (1967).
[10]J. Arvieux, Nucl. Phys. **A221**, 253 (1974).
[11]E. Huttel, W. Arnold, H. Baumgart, H. Berg, and G. Clausnitzer, Nucl. Phys. **A406**, 443 (1983); E. Huttel, W. Arnold, H. Berg, H. H. Krause, J. Ulbricht, and G. Clausnitzer, *ibid.* **A406**, 435 (1986).
[12]A. C. Phillips, Rep. Prog. Phys. **40**, 905 (1977).
[13]Y. Avishai and A. S. Rinat, Phys. Lett. **36B**, 161 (1971).
[14]W. Timm and M. Stingl, J. Phys. G **2**, 551 (1976).
[15]D. Eyre, A. C. Phillips, and F. Roig, Nucl. Phys. **A275**, 13 (1977).
[16]A. A. Kvitsinskii, Pis'ma Zh. Eksp. Teor. Fiz. **36**, 375 (1982) [JETP Lett. **36**, 455 (1982)].
[17]R. A. Malfliet and J. A. Tjon, Nucl. Phys. **A127**, 161 (1969); the actual parameters used are those given in Ref. 1.
[18]E. O. Alt, in *Proceedings of the VIIth International Conference on Few-Body Problems in Nuclear and Particle Physics,* edited by A. N. Mitra, I. Slaus, V. S. Bashin, and V. K. Gupta (North-Holland, Amsterdam, 1976), p. 76.
[19]J. L. Friar, B. F. Gibson, and G. L. Payne, Phys. Rev. C **28**, 983 (1983).
[20]H. Zankel and L. Mathelitsch, Phys. Lett. **132B**, 27 (1983).
[21]G. H. Berthold and H. Zankel, Phys. Rev. C **34**, 1203 (1986).
[22]L. Tomio, A. Delfino, and S. K. Adhikari, Phys. Rev. C **35**, 441 (1987).

[23]J. L. Friar, B. F. Gibson, G. L. Payne, and C. R. Chen, Phys. Rev. C **30**, 1121 (1984).
[24]C. R. Chen, G. L. Payne, J. L. Friar, and B. F. Gibson, Phys. Rev. C **33**, 401 (1986).
[25]A. A. Kvitsinskii and S. P. Merkuriev, Yad. Fiz. **41**, 647 (1985) [Sov. J. Nucl. Phys. **41**, 412 (1985)].
[26]Gy. Bencze, C. Chandler, J. L. Friar, A. G. Gibson, and G. L. Payne, Phys. Rev. C **35**, 1188 (1987).
[27]S. K. Adhikari and T. K. Das, Phys. Rev. C **37**, 1376 (1988).
[28]L. D. Faddeev, Zh. Eksp. Teor. Fiz. **39**, 1459 (1960) [Sov. Phys.—JETP **12**, 1014 (1961)].
[29]L. L. Foldy and W. Tobocman, Phys. Rev. **105**, 1099 (1957).
[30]H. P. Noyes, in *Three Body Problem in Nuclear and Particle Physics,* edited by J. S. C. McKee and P. M. Rolph (North-Holland, Amsterdam, 1970), p. 2.
[31]M. Abramowitz and I. A. Stegun, *Handbook of Mathematical Functions* (Dover, New York, 1972).
[32]P. M. Prenter, *Splines and Variational Methods* (Wiley, New York, 1975).
[33]W. M. Kloet and J. A. Tjon, Ann. Phys. (N.Y.) **79**, 407 (1973).
[34]G. L. Payne, W. H. Klink, W. N. Polyzou, J. L. Friar, and B. F. Gibson, Phys. Rev. C **30**, 1132 (1984).
[35]C. R. Chen, G. L. Payne, J. L. Friar, and B. F. Gibson, Phys. Rev. C **33**, 1740 (1986).
[36]L. M. Delves, Phys. Rev. **118**, 1318 (1960); W. T. H. van Oers and J. D. Seagrave, Phys. Lett. **24B**, 562 (1967); J. S. Whiting and M. G. Fuda, Phys. Rev. C **14**, 18 (1976).
[37]S. P. Merkuriev, A. A. Kvitsinsky, and V. V. Kostrykin, *Proceedings of the International Conference on the Theory of Few-Body and Quark-Hadronic Systems* (J.I.N.R., Dubna, U.S.S.R., 1987), p. 6.